Published OnlineFirst May 8, 2014; DOI: 10.1158/0008-5472.CAN-13-2893-T

Therapeutics, Targets, and Chemical Biology

Cancer Research

Targeting Mitochondrial Oxidative Metabolism in Melanoma Causes Metabolic Compensation through Glucose and Glutamine Utilization

Ji-Hong Lim[1,2,3], Chi Luo[1,2], Francisca Vazquez[1,2], and Pere Puigserver[1,2]

Abstract

Metabolic targets offer attractive opportunities for cancer therapy. However, their targeting may activate alternative metabolic pathways that can still support tumor growth. A subset of human melanomas relies on PGC1α-dependent mitochondrial oxidative metabolism to maintain growth and survival. Herein, we show that loss of viability caused by suppression of PGC1α in these melanomas is rescued by induction of glycolysis. Suppression of PGC1α elevates reactive oxygen species levels decreasing hypoxia-inducible factor-1α (HIF1α) hydroxylation that, in turn, increases its protein stability. HIF1α reprograms melanomas to become highly glycolytic and dependent on this pathway for survival. Dual suppression of PGC1α and HIF1α causes energetic deficits and loss of viability that are partially compensated by glutamine utilization. Notably, triple suppression of PGC1α, HIF1α, and glutamine utilization results in complete blockage of tumor growth. These results show that due to high metabolic and bioenergetic flexibility, complete treatment of melanomas will require combinatorial therapy that targets multiple metabolic components. *Cancer Res; 74(13); 3535–45. ©2014 AACR.*

Introduction

Cancer cells rely on activated metabolic routes to support cell proliferation and survival (1–3). The wiring and directional fluxes of these metabolic pathways is regulated through signaling/transcription mechanisms that are targets of oncogenic or tumor-suppressor activities (4–6). For example, the oncogene c-myc reprograms carbon metabolism toward the use of glutamine as a main substrate to maintain ATP levels and promote cell growth (7, 8). The fact that tumor cells are highly dependent on specific metabolic and energetic routes could be exploited to develop anticancer therapies (9, 10).

We recently found that a subset of human melanomas overexpress the transcriptional coactivator PGC1α that reprograms them to largely depend on mitochondrial oxidation for growth and survival (11). As a consequence, PGC1α-positive melanoma tumors and derived cell lines are more sensitive to mitochondrial inhibition (11, 12). On the other hand, PGC1α-negative melanoma cells rely more on glycolysis and are largely insensitive to suppression of mitochondrial metabolism. These studies suggest that although the subset of PGC1α-positive melanomas could be targeted by blocking mitochondrial oxidation, alternative metabolic pathways exist for melanoma growth that could compensate the inhibition of mitochondria metabolism.

The family of hypoxia-inducible transcription factors (HIF), which includes HIF1α, controls metabolic and cellular programs that support survival and tumorigenesis (13, 14). HIF1α regulation is largely due to hydroxylation of two proline residues (402 and 564) catalyzed by prolyl hydroxylases enzymes (PHD; ref. 15). Prolyl hydroxylation of HIF1α causes polyubiquitination through binding of the von Hippel–Lindau (VHL) protein, which is part of an E3 ligase complex, and degradation by the proteasome. The fact that PHDs' catalytic activity requires oxygen, iron, and 2-oxoglutarate makes these enzymes oxygen sensors that cause increased HIF1α stability under hypoxic conditions (16, 17). There is, however, HIF1α accumulation in normoxic conditions through increases in reactive oxygen species (ROS), 2-oxoglutarate analogs, or iron chelation, which suppress PHD enzymatic activity. HIF1α stability caused by changes in PHD activities is one of the major mechanisms by which HIF1α controls expression of gene programs, including glycolysis and angiogenesis, that promote tumor progression (18, 19). In addition, because HIF1α increases glycolytic fluxes it can function as a metabolic alternative pathway to maintain energetic and cellular tumor growth (20).

Many oncogenic signals drive bioenergetic requirements in tumor cells through increases in glucose metabolism. In some

Authors' Affiliations: [1]Department of Cancer Biology, Dana-Farber Cancer Institute; [2]Department of Cell Biology, Harvard Medical School, Boston, Massachusetts; and [3]Department of Biomedical Chemistry, College of Biomedical and Health Science, Konkuk University, Chungju, Chungbuk, Republic of Korea

Note: Supplementary data for this article are available at Cancer Research Online (http://cancerres.aacrjournals.org/).

J.-H. Lim and C. Luo contributed equally to this work.

Corresponding Author: Pere Puigserver, Dana-Farber Cancer Institute, 450 Brookline Avenue, CLSB-11144, Boston, MA 02215. Phone: 617-582-7977; Fax: 617-632-5363; E-mail: pere_puigserver@dfci.harvard.edu

doi: 10.1158/0008-5472.CAN-13-2893-T

Published OnlineFirst May 8, 2014; DOI: 10.1158/0008-5472.CAN-13-2893-T

tumor types or conditions, glutamine, the most abundant amino acid in blood, is utilized to promote tumor growth (7), and certain glucose PET–negative tumors exhibited high rates of glutamine consumption (21, 22). In cancer cells, intracellular glutamine exceeds the requirements for protein synthesis and is used for different metabolic activities, including ATP synthesis and lactate production, nucleotide, lipid, and glutathione synthesis (8). As a consequence of this metabolic and bioenergetic pleiotropy, glutamine is an important nutrient that supports tumor growth and survival (3, 6). In fact, glutaminase inhibitors have been shown to be potent inhibitors of several types of malignancies (23, 24). Glutamine is efficiently used for mitochondrial metabolism and is decoupled from glycolysis, providing an alternative bioenergetic and anabolic substrate (25).

Here, we report that inhibition of mitochondrial metabolism through suppression of PGC1α in melanomas results in the emergence of sequential metabolic and bioenergetic compensatory pathways that allow cell survival and tumor progression. The first compensation involves a ROS-dependent activation of HIF1α leading to increased glycolytic rates. Subsequent suppression of HIF1α results in an alternative metabolic compensation through increases in glutamine utilization that support melanoma growth and survival. Targeting PGC1α, HIF1α, and glutamine utilization is required to completely block tumor growth. In addition, we show that these alternative metabolic pathways are induced not only by exogenous perturbations but also selected naturally as alternative mechanisms for tumor growth. These results underscore the metabolic plasticity of cancer cells and show that a combinatorial therapy will be required to treat tumors using metabolic targets.

Materials and Methods

Reagents and antibodies

N-acetyl-L-cysteine, H_2O_2, amino acids, MG132, dimethyl-α-ketoglutarate, anti-HA, PEG-SOD, PEG-catalase, anti-FLAG, and Flag-M2 affinity beads were purchased from Sigma-Aldrich. Piperlongumine and Anti-PGC1α (H-300) were purchased from BioVision Research Products and Santa Cruz Biotechnology. Antibodies against cleaved caspase-3, 9, PARP, proline 564 hydroxylated HIF1α, and total HIF1α were purchased from Cell Signaling Technology. Anti-tubulin and lamin B antibodies were purchased from Millipore.

Cell culture and lentivirus production and infection

Melanoma cells were cultured in high-glucose DMEM with 5 mmol/L L-glutamine containing 10% FBS unless otherwise indicated. Lentiviruses were produced from HEK293T cells as previously described (26). Lentivirus particles were collected 48 hours after posttransfection and used to infect melanoma cells in the presence of 8 μg/mL polybrene, and then infected cells were selected with 2 μg/mL of puromycin or 7 μg/mL blasticidin for 4 days before experiments. Doxycycline inducible shRNA pLKO-expressing melanoma cells were incubated with doxycycline (100 ng/mL) before experiments. GFP control and Flag-HA-PGC1α adenovirus have been previously described (27).

Western blot analysis

Cells were lysed in a buffer containing 1% IGEPAL, 150 mmol/L NaCl, 20 mmol/L HEPES (pH, 7.9), 10 mmol/L NaF, 0.1 mmol/L EDTA, 1 mmol/L sodium orthovanadate and 1× protease inhibitor cocktail. Cell lysates were electrophoresed on SDS-polyacrylamide gels and transferred to Immobilon-P membrane (Millipore).

Quantitative real-time PCR

Total RNA was isolated with TRIzol (Invitrogen) and 2 μg of total RNA was used for cDNA synthesis using a High-Capacity cDNA Reverse Transcription Kit (Applied Biosystems). Quantitative real-time PCRs were carried out using SYBR Green PCR Master Mix (Applied Biosystems). Primers used for PCR are list in Supplementary Table S3.

Measurement of antioxidant activity

Infected cells were grown for 24 hours and cell extracts were used to measure human catalase, superoxide dismutase, and glutathione peroxidase activities. Enzymatic activities were measured according to the manufacturer's instructions (Cayman Chemical Company).

Clonogenic assay

For clonogenic assay, 1×10^4 melanoma cells were seeded in 6-well plate and maintained in the medium as indicated in individual experiment. After 7 days, cells in the plate were fixed by 10% formalin, followed by staining with crystal violet for 10 minutes.

Glutathione and NADPH level

The levels of NADPH, NADH+, reduced glutathione (GSH), and oxidized glutathione (GSSG) in cultured cells were determined using a NADP+/NADPH quantification Kit, Glutathione Colorimetric Detection Kit (BioVision), and OxiSelect Glutathione Assay Kit (Cell Biolabs), following the manufacturer's instructions. Briefly, cell lysates were prepared in an NADP+/NADPH extraction buffer, and then NADPH and NADP+ levels were measured by spectrometry at OD 450 nm. For measurement of glutathione levels, cell lysates were prepared in extraction buffer without thiol compounds such as dithiothreitol (DTT) or β-mercaptoethanol, and then glutathione levels were measured by spectrometry at OD 405 nm.

Glucose consumption, lactate production, glutamine consumption, and ATP levels

Lactate, glucose, and glutamine assay kits (BioVision Research Products) were used to measure extracellular lactate, glucose, and glutamine following the manufacturer's instructions. Briefly, equal number of cells were seeded in 6-well plates and cultured in phenol-red–free DMEM for 24 hours. For glutamine assay, cells were cultured with 1 mmol/L glutamine and 25 mmol/L glucose containing phenol-red–free DMEM. Intracellular ATP levels were determined in cell lysates using a luciferin–luciferase–based ATP Determination Kit (Invitrogen) according to the manufacturer's instructions, and all values were normalized to cellular protein concentration.

Published OnlineFirst May 8, 2014; DOI: 10.1158/0008-5472.CAN-13-2893-T

Tumor xenograft assay

A375P cells (1×10^6) stably expressing the indicated shRNAs were injected subcutaneously into the flank of nude mice (Taconic) in 100 μL of media. Ten days after cell injection, mice were housed with 2 mg/mL of doxycycline and 5% of sucrose containing water until the end of the experiment. For the small-molecule treatments, 20 days after cell injection, mice were injected daily with piperlongumine (1 mg/kg), compound 968 (150 μg), or DMSO for 10 days. Tumor volumes were monitored with a caliper and calculated using the equation: volume $= ab^2/2$, where a is the maximal width and b is maximal orthogonal width. All procedures were conducted in accordance with the guidelines of the Beth Israel Deaconess Medical Center Institutional Animal Care and Use Committee.

Outside of tumors contained nonnecrotic area were used for isolation of nucleus extracts, and then nucleus extracts were used to measure HIF1α levels.

In vitro hydroxylation

GST-tagged HIF1α ODDD (oxygen-dependent degradation domain) and full-length PHD2 proteins were expressed in *Escherichia coli* BL21 cells and A375P cells, and proteins were purified using GSH-affinity chromatography and HA-affinity beads. For the *in vitro* proline hydroxylation assay, GST-ODDD (100 ng) was incubated with A375P cell–derived PHD2 (50 ng) at 30°C for 1 hour in a reaction buffer containing 40 mmol/L Tris–HCl, pH 7.4, 4 mmol/L 2-oxoglutarate, 1.5 mmol/L $FeSO_4$, 10 mmol/L KCl, and 3 mmol/L $MgCl_2$. The hydroxylation at the Pro 564 residue was analyzed by immunoblotting using an anti-Pro564 (OH) antibody.

^{14}C-L-glutamine oxidation assay

Scrambled, PGC1α, or HIF1α shRNA stably expressing A375P cells were cultured for 48 hours with 2 mmol/L glutamine and 25 mmol/L glucose-containing DMEM. At this time, medium was changed with 1 mmol/L L-glutamine and 25 mmol/L glucose-containing DMEM, and cells were further incubated for 12 hours. Then, cells were incubated with 2 μCi/mL of ^{14}C-L-glutamine (PerkinElmer) for 3 hours. ^{14}C-labeled CO_2 was captured in phenylethylamine-soaked Whatman paper and measured on a scintillation counter.

GSEA analysis

A previously published gene expression profile of A375P cells stably expressing control shRNAs or two different shRNAs against PGC1α (GSE7553) was analyzed with the GSEA algorithm. Thirteen gene sets generated from cells exposed to hypoxia from MsigDB (shown in Supplementary Table S1) were tested for enrichment in the PGC1α-suppressed cells using the default parameters.

Results

PGC1α suppress HIF1α protein stability and glycolysis in melanoma cell lines and tumors

We have recently shown that PGC1α is strongly overexpressed in a subset of melanoma tumors and derived cell lines (11). Depletion of PGC1α in these melanoma cells using a lentivirus encoding a targeting shRNA caused a decrease in cell viability as well as clonogenic cell survival (Fig. 1A). Although approximately 20% of the cells with suppressed PGC1α died from apoptosis, the cells that survived could be grown for a long term. These PGC1α-depleted surviving cells had only a slightly reduced growth rate compared with control cells, despite maintaining PGC1α levels suppressed (Fig. 1A, top right). The surviving PGC1α-suppressed cells displayed a reduction in mitochondrial oxidative phosphorylation but increased glycolysis and lactate production (11), suggesting that a metabolic switch to glycolysis might be an underlying mechanism that rescued viability. Because HIF1α promotes glycolysis, we probed the protein stability of this transcription factor. Figure 1B shows that HIF1α protein levels were strongly increased after shRNA-mediated PGC1α suppression in three PGC1α-positive melanoma cell lines. HIF1α reporter luciferase activity was accordingly elevated in these melanoma cell lines (Fig. 1C). The effect of PGC1α shRNAs on HIF1α protein stability was efficiently rescued by ectopic expression of PGC1α (Fig. 1D). In addition, when melanoma cells were grown *in vivo* as xenografts, the increase in HIF1α protein levels after PGC1α suppression was maintained (Fig. 1E). Consistent with HIF1α elevation, expression arrays performed after suppression of PGC1α (GSE7553) showed an enrichment of hypoxia-induced signatures in PGC1α-depleted compared with control melanoma cells (Fig. 1F). Specifically, 11 out of the 13 interrogated hypoxia-induced gene sets from MsigDB were enriched in PGC1α-depleted cells (Supplementary Table S1). In agreement with this observation, qPCR analysis showed that HIF1α target genes, including genes encoding for enzymes or proteins linked to glycolysis and lactate production, were increased upon PGC1α suppression in melanoma cell lines (Figs. 1G and Supplementary Fig. S1B) and xenografted tumors (Fig. 1H). In contrast and as predicted, PGC1α target genes, including mitochondrial oxidative phosphorylation and ROS detoxification genes, were substantially decreased (Supplementary Fig. S1A). Functionally, increases in HIF1α target genes caused by knockdown of PGC1α in cell lines and tumors resulted in increased glucose uptake and lactate production (Fig. 1I and J). Taken together, these results indicate that suppression of PGC1α results in metabolic and energetic compensation through increases in HIF1α protein stability and glycolysis.

PGC1α expression causes reduction of HIF1α protein stability through suppression of ROS production

As part of the oxidative metabolism program, suppression of PGC1α results in an increase in intracellular levels of ROS (11). Elevated ROS levels are one of the mechanisms whereby HIF1α protein is stabilized in normoxic conditions (28, 29). We used the antioxidant N-acetyl cysteine (NAC) to determine whether PGC1α suppression-dependent HIF1α protein stability was a result of increased ROS levels (30). Figure 2A shows that increased concentrations of NAC were sufficient to efficiently block HIF1α protein stability in PGC1α-suppressed A375P cells. Blockage of HIF1α induction in these cells translated in a reduction in their ability to induce

Published OnlineFirst May 8, 2014; DOI: 10.1158/0008-5472.CAN-13-2893-T

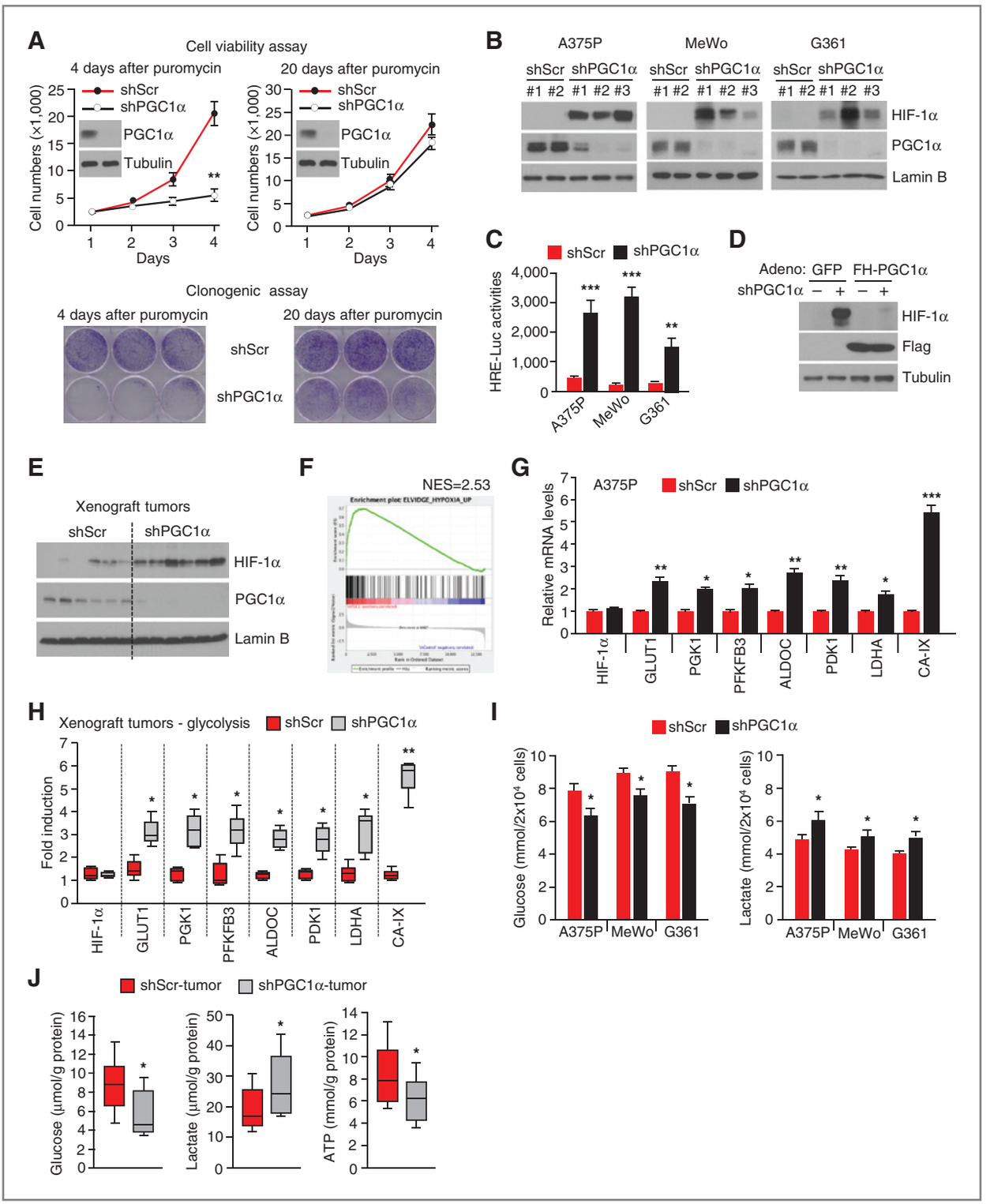

Figure 1. HIF1α levels and stability in PGC1α-suppressed cells. A, growth curve and clonogenic cell survival of A375P cells with transient (4 days) or chronic (20 days) PGC1α suppression. B and C, chronic suppression of PGC1α elevates HIF1α protein expression and transcriptional activities in melanoma cells. D, HIF1α levels after rescue of PGC1α expression in PGC1α-suppressed A375P cells. Mouse Flag-tagged PGC1α was expressed exogenously using adenoviruses for 24 hours before harvesting. E, HIF1α levels in A375P xenografts. F, GSEA enrichment plot for the top-scoring gene set. (*Continued on the following page.*)

Published OnlineFirst May 8, 2014; DOI: 10.1158/0008-5472.CAN-13-2893-T

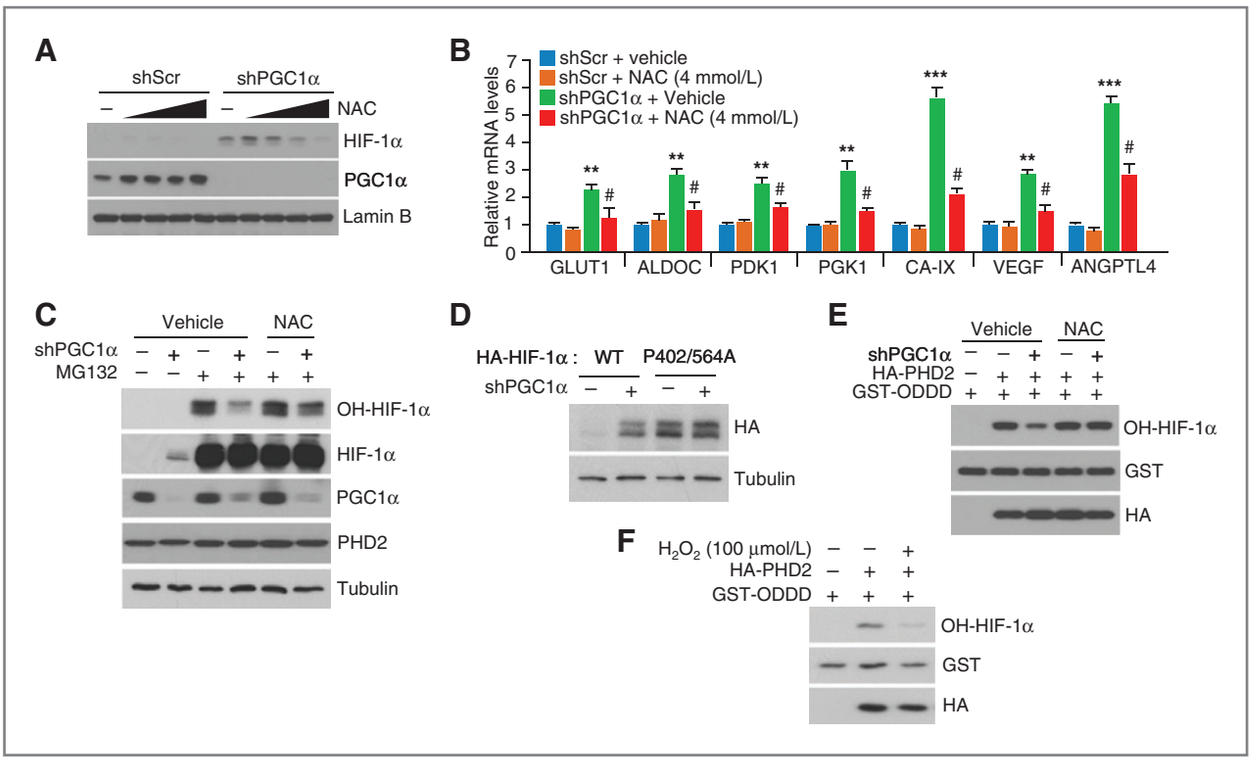

Figure 2. PGC1α suppression enhances the stability of HIF1α through increasing ROS levels. A, NAC blocks HIF1α accumulation induced by PGC1α suppression. PGC1α-depleted A375P cells were incubated with NAC (0.5, 1, 2, or 4 mmol/L) for 48 hours, and then whole-cell lysates were used to measure HIF1α protein levels. B, NAC attenuates the induction of HIF1α glycolytic target genes after PGC1α suppression. Total RNA was isolated from PGC1α-depleted A375P cells incubated with 4 mmol/L of NAC for 48 hours. C, proline hydroxylation of HIF1α is decreased in PGC1α-suppressed melanoma cells. PGC1α-suppressed A375P cells were incubated with 4 mmol/L NAC or vehicle for 48 hours, followed by incubation with 20 μmol/L of MG132 or DMSO for 3 hours before harvesting. D, HIF1α P402/564A mutant is not further stabilized after PGC1α suppression. E and F, oxidative stress induced by PGC1α depletion (E) or H_2O_2 (F) inhibits PHD2 enzymatic activity. Values represent mean ± SD of three independent experiments performed in triplicate; **, $P < 0.01$; and ***, $P < 0.001$ versus control shRNA; and #, $P < 0.05$ versus PGC1α shRNA.

glycolytic and angiogenic HIF1α target genes (Fig. 2B). We have recently shown that PGC1α levels define the metabolic state of melanomas (11). Interestingly, endogenous PGC1α levels also modulated the magnitude of induction of HIF1α protein stability in response to either hypoxia or ROS increases through hydrogen peroxide treatment, with a more robust induction of HIF1α protein in PGC1α-negative cell lines (Supplementary Fig. S2A–S2C). As expected, the induction of HIF1α target genes in response to hypoxia or hydrogen peroxide was also more significant in PGC1α-negative cell lines (Supplementary Fig. S2D and S2E). These results suggest that melanomas also select or switch to the HIF1α-dependent alternative metabolic route in their natural history.

HIF1α protein stability is regulated through prolyl hydroxylation of residues 402 and 564 (15). To determine whether ROS-induced HIF1α stability in melanoma cells was due to changes in prolyl hydroxylation, we measured this chemical modification using specific antibodies. Figure 2C shows a decrease in HIF1α prolyl hydroxylation in the presence of the proteasome inhibitor MG132 upon suppression of PGC1α. However, this decrease was substantially prevented by treatment with the antioxidant NAC. Moreover, in contrast with the stability of wild-type HIF1α protein, a defective HIF1α proline hydroxylation mutant (P402/564A) showed no changes in protein stability after PGC1α suppression (Fig. 2D). The fact that knockdown of PGC1α increased HIF1α protein stability and decreased prolyl hydroxylation suggests that the enzymatic activity of PHD2 was decreased. To test this possibility, we immunoprecipitated PHD2 from control and PGC1α shRNA melanoma cell lines and measured the PHD activity using recombinant HIF1α as a substrate (31). Figure 2E shows

(*Continued.*) Gene expression profile of A375P cells stably expressing control shRNAs or two different shRNAs against PGC1α (GSE7553) was analyzed with the GSEA algorithm for enrichment of gene sets related to hypoxia. G, expression of HIF1α glycolytic targets after PGC1α knockdown. H, HIF1α glycolytic target genes are increased in PGC1α-depleted tumors. I, glucose utilization and lactate production in PGC1α-depleted melanoma cells. J, glucose utilization, lactate production, and ATP levels in PGC1α-depleted tumors. Values represent mean ± SD of three independent experiments performed in triplicate; *, $P < 0.05$; **, $P < 0.01$; and ***, $P < 0.001$ versus control shRNA. The whiskers in the box plots represent the maximum and the minimum value.

Published OnlineFirst May 8, 2014; DOI: 10.1158/0008-5472.CAN-13-2893-T

that PHD2 enzymatic activity was decreased in PGC1α-suppressed melanoma cells, but this activity was rescued by NAC treatment. In addition, hydrogen peroxide mimicked the effects of PGC1α suppression, decreasing PHD2 activity (Fig. 2F).

Taken together, these results suggest that suppression of PGC1α induces HIF1α protein stability through induction of ROS levels and activation of PHD2 enzymatic activity in melanoma cells.

HIF1α maintains survival and compensates metabolic and energetic PGC1α function in melanoma cells and tumors

As illustrated in Fig. 1I, elevated levels of HIF1α upon suppression of PGC1α result in a metabolic reprogramming toward a more glycolytic metabolism. These results suggested that these cells might now depend on HIF1α to maintain their energetic status and survival. To assess this possibility, we suppressed HIF1α in PGC1α knockdown cells using a doxycycline-inducible shRNA. Figure 3C shows that both PGC1α and HIF1α levels were efficiently suppressed after doxycycline treatment and HIF1α targets were decreased (Fig. 3A). Of note, doxycycline did not have any effect on the expression of HIF1α targets in control cells (Supplementary Fig. S3A). Double knockdown of PGC1α and HIF1α substantially reduced cell viability (Fig. 3B, left) and clonogenic cell survival (Fig. 3B right panel), which correlated with increased apoptotic markers, including cleavages of caspase-9 and PARP (Fig. 3C), and decreased intracellular ATP levels (Fig. 3E). Interestingly, inhibition of glucose utilization by 2-deoxy-glucose led to reduced viability (Fig. 3D), mimicking the effect caused by HIF1α suppression in PGC1α-depleted cells; therefore, HIF1α depletion in these cells caused apoptosis, at least in part, through inhibition of the glycolytic flux. In addition, consistent with HIF1α increase, hypoxia partially rescued cell death induced by acute PGC1α knockdown (Supplementary Fig. S3B), further supporting the protective role of HIF1α for cell survival upon metabolic stress. Next, to test how double HIF1α/PGC1α depletion decreased cell survival, we measured changes in metabolites and enzymes associated with ROS activities. Double HIF1α and PGC1α knockdown in A375P cells did not change NADPH and glutathione levels (Supplementary Fig. S3C), ROS detoxification gene expression (Supplementary Fig. S3D and S3F), ROS levels (Supplementary Fig. S3E), or antioxidant enzymatic activities (Supplementary Fig. S3G). Moreover, addition of polyethylene glycol (PEG)–conjugated superoxide dismutase or catalase, which repress intracellular oxidative stress (Supplementary Fig. S3H), failed to rescue cell viability in PGC1α- and HIF1α-suppressed melanoma cells (Supplementary Fig. S3I). Altogether, these results suggest that the loss of viability in double HIF1α/PGC1α-suppressed cells is not triggered by an increase in ROS levels and is likely due to a failure to maintain cellular energy levels.

To determine the effects of the double PGC1α/HIF1α knockdown in tumor maintenance, we injected cells expressing PGC1α shRNA and inducible HIF1α shRNA into nude mice and allowed the tumors to form before the induction of the HIF1α shRNA with doxycycline. Although, suppression of HIF1α alone did not compromise the growth of the cells *in vitro*, there was an effect on tumor growth after the tumor reached approximately 500 mm^3 in size (Fig. 3F). Consistent with our previous results, PGC1α suppression resulted in a decrease in tumor growth. However, double knockdown of PGC1α/HIF1α had a more pronounced effect on the growth of the tumor. The effects observed on tumor growth were consistent, with substantial decreases in the expression of glycolytic and angiogenic genes (Fig. 3G) and on ATP levels (Fig. 3H). These results indicate that suppression of PGC1α causes a HIF1α-dependent bioenergetic switch toward glycolysis. Moreover, these results show that simultaneously targeting the PGC1α and HIF1α arms results in a more pronounced effect on cell survival and tumor growth than targeting either arm alone.

We have recently shown that suppression of PGC1α sensitizes melanoma tumors to ROS-inducing drugs such as piperlongumine (11). Because levels of antioxidant enzymes were decreased to the same extent in single PGC1α and double PGC1α- and HIF1α-suppressed cells, we determined whether increasing ROS levels would further reduce the growth of these tumors. Notably, piperlongumine completely prevented tumor growth of the double PGC1α and HIF1α-depleted cells (Fig. 3I and Supplementary Fig. S3J), which correlated with increased apoptosis markers (Supplementary Fig. S3K). In aggregate, these results indicate that ROS-inducing drugs will be very efficient in melanoma tumors in which PGC1α and HIF1α are inhibited.

Glutamine utilization maintains survival and compensates metabolic and energetic HIF1α and PGC1α function in melanoma cells and tumors

Despite the reduction of oxidative and glycolytic metabolism, PGC1α- and HIF1α-suppressed cells were able to grow, albeit to a slower rate, and form small tumors. To investigate the energetic source that contributed to the growth of these cells, we exposed them to single-carbon sources and measured their ability to prevent apoptosis. Figure 4A shows that glucose and branched-chain amino acids were unable to block apoptosis, shown by the levels of caspases or PARP cleavage. Other carbon sources, including glutamate, pyruvate, and TCA intermediates, attenuated the levels of apoptotic markers. Strikingly, however, glutamine dramatically prevented the induction of these apoptotic markers to undetectable levels. Reduction in apoptosis correlated with increased cell number (Fig. 4B), elevated levels of intracellular ATP (Fig. 4C), and clonogenic cell survival (Fig. 4D), which was more pronounced in PGC1α/HIF1α-suppressed cells than in control cells. To further explore the role of glutamine in melanoma cell viability, we used a specific glutaminase inhibitor, compound 968 (24). Consistent with the effect of glutamine promoting cell survival in PGC1α- and HIF1α-suppressed cells, the 968 glutaminase inhibitor caused a substantial reduction in cell number and ATP levels (Fig. 4E). Next, we used ^{14}C-glutamine to investigate the rates of glutamine utilization after depletion of PGC1α/HIF1α. In contrast with the increase in glucose utilization (Fig. 1I and J), PGC1α-suppressed cells exhibited a decrease in glutamine utilization measured as release (Fig. 4F) and uptake

Published OnlineFirst May 8, 2014; DOI: 10.1158/0008-5472.CAN-13-2893-T

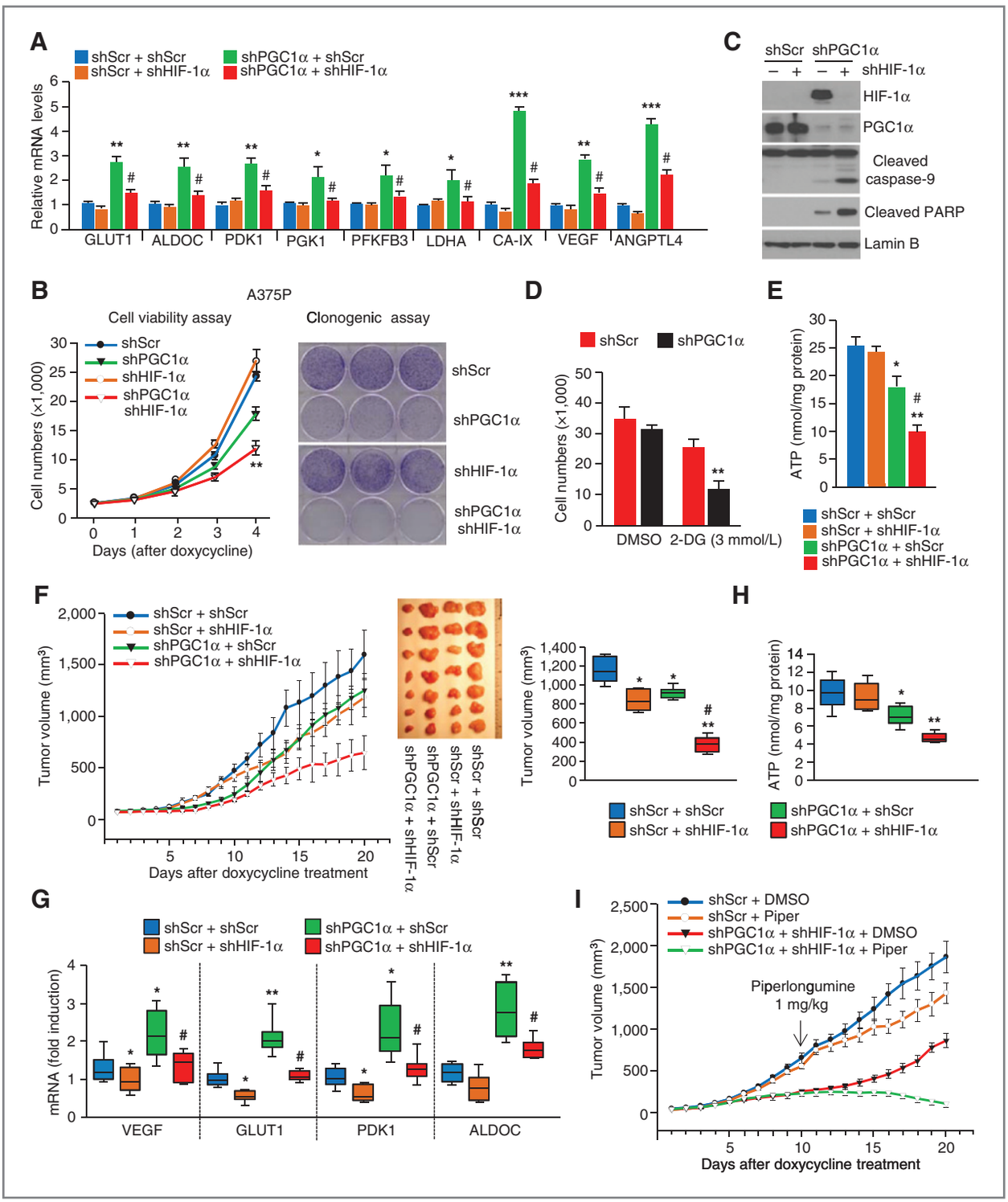

Figure 3. PGC1α-suppressed melanoma cells are dependent on HIF1α expression. A, expression of glycolytic genes after HIF1α and PGC1α suppression in A375P cells. B, growth curve and clonogenic cell survival of HIF1α- and PGC1α-suppressed A375P cells. C, detection of apoptosis in HIF1α- and PGC1α-suppressed A375P cells. D, cell growth after 2-deoxy-glucose (2DG) treatment in PGC1α-suppressed A375P cells. E, ATP levels in HIF1α- and PGC1α-suppressed A375P cells. F, tumor growth after suppression of PGC1α and HIF1α. The tumor growth curves are plotted as mean ± SEM ($n = 10$). G, inhibition of HIF1α decreases glycolytic gene expression induced by PGC1α depletion in tumors. H, inhibition of HIF1α decreases ATP levels in PGC1α-depleted tumors. I, effect of piperlongumine in HIF1α- and PGC1α-suppressed tumors. Mice were daily injected with piperlongumine (1 mg/kg) or DMSO for 10 days as described in Materials and Methods ($n = 8$). Values represent mean ± SD of three independent experiments performed in triplicate; *, $P < 0.05$; **, $P < 0.01$; and ***, $P < 0.001$ versus control shRNA and #, $P < 0.05$ versus PGC1α shRNA. The whiskers in the box plots represent the maximum and the minimum value.

Published OnlineFirst May 8, 2014; DOI: 10.1158/0008-5472.CAN-13-2893-T

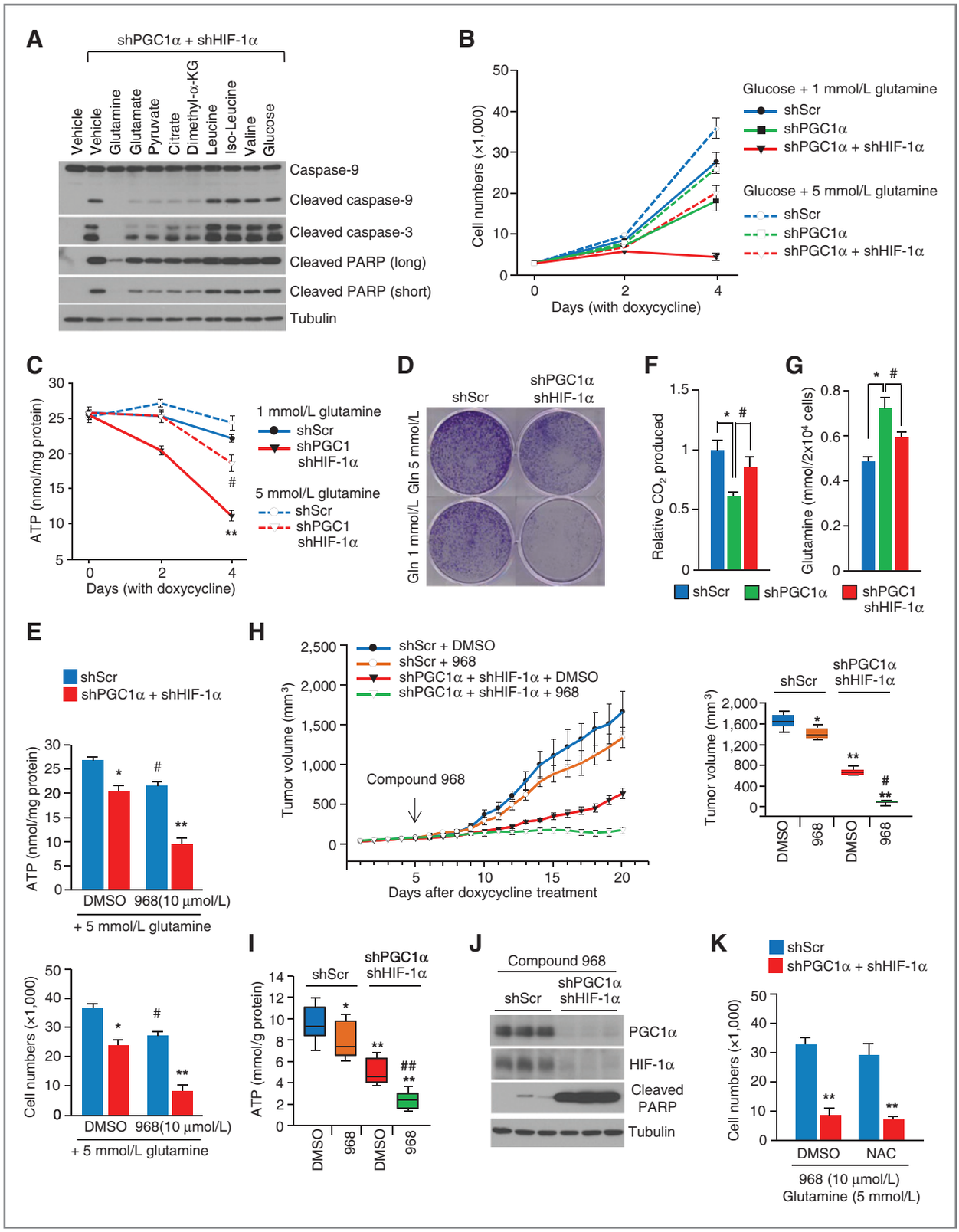

Figure 4. Glutamine utilization after PGC1α and HIF1α suppression. A, apoptosis in double PGC1α/HIF1α-suppressed cells after exposure to the indicated nutrients. A375P cells expressing PGC1α shRNA and a doxycycline-inducible shRNA against HIF1α were incubated for 4 days with 100 ng/mL doxycycline and 5 mmol/L glutamine, 25 mmol/L glucose, or 2 mmol/L of the indicated amino acids or metabolites. (*Continued on the following page.*)

Published OnlineFirst May 8, 2014; DOI: 10.1158/0008-5472.CAN-13-2893-T

(Fig. 4G) of $^{14}CO_2$. However, PGC1α/HIF1α-suppressed cells increased the levels of glutamine utilization (Fig. 4F) and uptake (Fig. 4G).

To further support the relevance of glutamine utilization *in vivo*, we treated mice xenografted with PGC1α or PGC1α/HIF1α-suppressed cells with the 968 glutaminase inhibitor. Figure 4H shows that 968 had a small effect on the growth of control tumors but largely prevented tumor growth of PGC1α/HIF1α-suppressed xenografts. The effects seen on tumor growth correlated with strong reduction of ATP levels (Fig. 4I) and the induction of cell death markers (Fig. 4J). Because inhibition of glutamine utilization also increases ROS levels, we tested whether reduced cell viability by glutaminase inhibitor depends on ROS accumulation. Figure 4K shows that NAC does not rescue cell viability upon glutaminase inhibitor, suggesting that glutamine utilization conferring resistance to apoptosis induced by PGC1α/HIF1α suppression is independent of ROS. Together, these results indicate that glutamine is an alternative energy source to maintain cell survival in melanoma tumors, particularly in conditions in which mitochondrial metabolism and glycolysis are reduced.

Discussion

In this study, we report that melanomas develop alternative metabolic compensatory strategies for survival and growth. Inhibition of mitochondrial metabolism through suppression of PGC1α expression in highly oxidative cells results in elevation of ROS levels, triggering an increase in HIF1α stability and rewiring toward glycolysis. Subsequent inactivation of HIF1α reactivates glutamine utilization to maintain the cellular bioenergetic state that is necessary for survival after inhibition of oxidative phosphorylation and glycolysis. These results reveal three alternative compensatory metabolic/bioenergetic routes, PGC1α and mitochondrial oxidative phosphorylation, HIF1α and glycolysis, and glutamine utilization, underscoring the flexibility of cellular metabolism in melanomas and possibly other tumors.

Cellular metabolism has evolved to be highly flexible and rapidly rewired to adapt to nutrient and energy fluctuations. For example, in fasting conditions skeletal muscle or liver cells quickly switch to utilize fatty acids instead of glucose as an energy source (32). Similar metabolic flexibilities occur in cancer cells that reprogram their metabolism to meet high bioenergetic and biosynthetic demands to proliferate and survive in disparate nutrient and hypoxic conditions (3, 33). In cancer cells, such metabolic and energetic rewiring is the result of both genetic changes and nongenetic adaptations, similar to the adaptations occurring in liver or skeletal muscle. The abundance of alternative pathways and the existence of these nongenetic adaptations make it difficult to exploit metabolic targets for cancer therapy, and it remains unclear that targeting a single metabolic component could be an effective anticancer therapy. Our results provide experimental evidence of these nongenetic adaptations when targeting critical metabolic pathways in melanomas and show that, in this context, targeting a single metabolic node is not sufficient to cause a robust response. Fortunately, it is likely that the number of alternative metabolic pathways that the cancer cell can use is limited and that rational combination therapy targeting all possible nodes could maximize the effect of the treatment. Our results provide an example of such rational combination therapy and show that by blocking all key metabolic nodes it is possible to elicit a robust response.

A major cellular function of PGC1α is to promote mitochondrial biogenesis and to increase the cellular energetic state while in parallel strongly protecting against oxidative stress. A subset of melanoma tumors (and likely other tumor types) overexpresses PGC1α that drives augmented mitochondrial oxidative phosphorylation and ROS detoxification capacities. This subset of tumors largely depends on PGC1α for growth and survival and is more resistant to oxidative stress (11). Because mitochondrial oxidation generates ROS, the PGC1α-mediated increase in ROS detoxification enzymes is essential to maintain survival. In addition, this augmented ROS detoxification capacity facilitates the cell's oxidative phosphorylation function as elevated ROS levels suppress ATP synthesis (34). This is clearly exemplified by the higher resistance of PGC1α-positive melanoma tumors to ROS-inducing drugs (11). Increased sensitivity to ROS after PGC1α suppression is partially counterbalanced by the induction of HIF1α protein stability that maintains the bioenergetic state and survival of the cells. This is consistent with the reported protective effects of HIF1α in many tumors types (13) and with our data showing that ROS-inducing drugs are more effective after double suppression of PGC1α and HIF1α.

Low concentrations of oxygen are the main signal to increase HIF1α protein stability. However, under normoxic conditions increases in ROS levels can also result in elevated HIF1α protein stability (18, 35, 36). Our results show that PGC1α suppression results in ROS-mediated increase in HIF1α protein stability largely mediated through inhibition of PHD2. Although the mechanisms whereby ROS decreases PHD2 activity are unknown, our data suggest that PHD2

(*Continued.*) B–D, growth curves (B), ATP levels (C), and clonogenic cell survival (D) in PGC1α/HIF1α double-knockdown A375P cells after exposure to different concentrations of glutamine. E, cell growth and ATP levels after pharmacologic inhibition of glutamine utilization in PGC1α/HIF1α double-knockdown A375P cells. Cells were incubated with doxycycline, 5 mmol/L glutamine, and 25 mmol/L glucose in the absence or presence of 10 μmol/L of compound 968 for 4 days as indicated. F, glutamine oxidation in PGC1α/HIF1α double-knockdown A375P cells. Cells were incubated with 1 mmol/L glutamine and ^{14}C-L-glutamine for 3 hours, and then ^{14}C-labeled CO_2 was measured. G, glutamine utilization in PGC1α/HIF1α double-knockdown A375P cells. H, the effects of glutamine utilization inhibition on tumor growth. Fifteen days after injection, mice were injected daily with compound 968 or DMSO and the tumor volume was measured ($n = 8$). I and J, ATP levels (I) and apoptosis (J) in PGC1α/HIF1α double-depleted tumors described in H. K, NAC does not rescue the growth of PGC1α/HIF1α double-knockdown A375P cells upon inhibition of glutamine utilization. Values represent mean ± SD of three independent experiments performed in triplicate; **, $P < 0.01$; $^{\#}$, $P < 0.05$; the whiskers in the box plots represent the maximum and the minimum value.

Published OnlineFirst May 8, 2014; DOI: 10.1158/0008-5472.CAN-13-2893-T

posttranslational modifications and/or differential protein interactions might account for the changes in enzymatic activity. In addition to the HIF1α increase after PGC1α suppression, our work also shows that natural PGC1α-negative melanoma tumors have an increased sensitivity to induction of HIF1α protein stability, suggesting that targeting PHD2 to inhibit HIF1α protein stability and compromise energy metabolism could be particularly effective in PGC1α-negative melanoma tumors.

In clinical settings, PET-negative tumors tend to be positive for glutamine utilization, suggesting that glutamine, instead of glucose, is their main nutrient source (21). It is known that some mutational events drive tumors toward the use of glutamine (7, 8). Our results suggest that suppression of glucose metabolism by drug treatments could also result in a rewiring toward the use of glutamine. Under these conditions, glutaminase inhibitors could be used in combination therapy. The mechanism by which glutamine utilization rescues cell death caused by dual inhibition of PGC1α and HIF1α is unknown. Enhanced glutamine oxidation as observed in our studies is likely to be one mechanism. In addition, reductive glutamine metabolism that can either increase fatty acid synthesis, as reported to occur under hypoxic conditions (37), or change the α-ketoglutarate/citrate ratio (38), might also contribute to melanoma survival after PGC1α and HIF1α suppression.

In summary, our studies reveal a series of metabolic compensatory mechanisms that occur in melanoma and denote the energetic versatility and plasticity that these cells exhibit. These metabolic nodes could be targets for combinatorial cancer therapy.

Disclosure of Potential Conflicts of Interest

No potential conflicts of interest were disclosed.

Authors' Contributions

Conception and design: J.-H. Lim, F. Vazquez, P. Puigserver
Development of methodology: J.-H. Lim
Acquisition of data (provided animals, acquired and managed patients, provided facilities, etc.): C. Luo
Analysis and interpretation of data (e.g., statistical analysis, biostatistics, computational analysis): J.-H. Lim, C. Luo, F. Vazquez, P. Puigserver
Writing, review, and/or revision of the manuscript: J.-H. Lim, C. Luo, F. Vazquez, P. Puigserver
Study supervision: P. Puigserver

Acknowledgments

The authors thank Dr. Jong-Wan Park (Seoul National University, College of Medicine) who kindly provided HIF1α–related constructs.

Grant Support

J.-H. Lim was supported in part by a postdoctoral fellowship from the American Heart Foundation (13POST14750008) as well as a faculty research fund from Konkuk University, South Korea. These studies were funded in part by the Claudia Adams Barr Program in Cancer Research and Dana-Farber Cancer Institute funds.

The costs of publication of this article were defrayed in part by the payment of page charges. This article must therefore be hereby marked *advertisement* in accordance with 18 U.S.C. Section 1734 solely to indicate this fact.

Received October 7, 2013; revised March 18, 2014; accepted April 3, 2014; published OnlineFirst May 8, 2014.

References

1. Vander Heiden MG, Cantley LC, Thompson CB. Understanding the Warburg effect: the metabolic requirements of cell proliferation. Science 2009;324:1029–33.
2. Lunt SY, Vander Heiden MG. Aerobic glycolysis: meeting the metabolic requirements of cell proliferation. Annu Rev Cell Dev Biol 2011;27:441–64.
3. Ward PS, Thompson CB. Metabolic reprogramming: a cancer hallmark even Warburg did not anticipate. Cancer Cell 2012;21:297–308.
4. Kroemer G, Pouyssegur J. Tumor cell metabolism: cancer's Achilles' heel. Cancer Cell 2008;13:472–82.
5. Levine AJ, Puzio-Kuter AM. The control of the metabolic switch in cancers by oncogenes and tumor suppressor genes. Science 2010;330:1340–4.
6. Schulze A, Harris AL. How cancer metabolism is tuned for proliferation and vulnerable to disruption. Nature 2012;491:364–73.
7. Wise DR, Thompson CB. Glutamine addiction: a new therapeutic target in cancer. Trends Biochem Sci 2010;35:427–33.
8. Le A, Lane AN, Hamaker M, Bose S, Gouw A, Barbi J, et al. Glucose-independent glutamine metabolism via TCA cycling for proliferation and survival in B cells. Cell Metab 2012;15:110–21.
9. Butler EB, Zhao Y, Munoz-Pinedo C, Lu J, Tan M. Stalling the engine of resistance: targeting cancer metabolism to overcome therapeutic resistance. Cancer Res 2013;73:2709–17.
10. Zhao Y, Butler EB, Tan M. Targeting cellular metabolism to improve cancer therapeutics. Cell Death Dis 2013;4:e532.
11. Vazquez F, Lim JL, Chim H, Bhalla K, Girnun G, Pierce K, et al. PGC1a expression defines a subset of human melanoma tumors with increased mitochondrial capacity and resistance to oxidative stress. Cancer Cell 2013;23:287–301.
12. Haq R, Shoag J, Andreu-Perez P, Yokoyama S, Edelman H, Rowe GC, et al. Oncogenic BRAF regulates oxidative metabolism via PGC1alpha and MITF. Cancer Cell 2013;23:302–15.
13. Giaccia A, Siim BG, Johnson RS. HIF-1 as a target for drug development. Nat Rev Drug Discov 2003;2:803–11.
14. Semenza GL. Targeting HIF-1 for cancer therapy. Nat Rev Cancer 2003;3:721–32.
15. Schofield CJ, Ratcliffe PJ. Oxygen sensing by HIF hydroxylases. Nat Rev Mol Cell Biol 2004;5:343–54.
16. Jaakkola P, Mole DR, Tian YM, Wilson MI, Gielbert J, Gaskell SJ, et al. Targeting of HIF-alpha to the von Hippel-Lindau ubiquitylation complex by O2-regulated prolyl hydroxylation. Science 2001;292:468–72.
17. Ivan M, Kondo K, Yang H, Kim W, Valiando J, Ohh M, et al. HIFalpha targeted for VHL-mediated destruction by proline hydroxylation: implications for O2 sensing. Science 2001;292:464–8.
18. Kaelin WG Jr, Ratcliffe PJ. Oxygen sensing by metazoans: the central role of the HIF hydroxylase pathway. Mol Cell 2008;30:393–402.
19. Fong GH, Takeda K. Role and regulation of prolyl hydroxylase domain proteins. Cell Death Differ 2008;15:635–41.
20. Brahimi-Horn MC, Bellot G, Pouyssegur J. Hypoxia and energetic tumour metabolism. Curr Opin Genet Dev 2011;21:67–72.
21. Lieberman BP, Ploessl K, Wang L, Qu W, Zha Z, Wise DR, et al. PET imaging of glutaminolysis in tumors by 18F-(2S,4R)4-fluoroglutamine. J Nucl Med 2011;52:1947–55.
22. Rajagopalan KN, DeBerardinis RJ. Role of glutamine in cancer: therapeutic and imaging implications. J Nucl Med 2011;52:1005–8.
23. Seltzer MJ, Bennett BD, Joshi AD, Gao P, Thomas AG, Ferraris DV, et al. Inhibition of glutaminase preferentially slows growth of glioma cells with mutant IDH1. Cancer Res 2010;70:8981–7.
24. Wang JB, Erickson JW, Fuji R, Ramachandran S, Gao P, Dinavahi R, et al. Targeting mitochondrial glutaminase activity inhibits oncogenic transformation. Cancer Cell 2010;18:207–19.
25. Filipp FV, Ratnikov B, De Ingeniis J, Smith JW, Osterman AL, Scott DA. Glutamine-fueled mitochondrial metabolism is decoupled from glycolysis in melanoma. Pigment Cell Melanoma Res 2012;25:732–9.

Published OnlineFirst May 8, 2014; DOI: 10.1158/0008-5472.CAN-13-2893-T

26. Moffat J, Grueneberg DA, Yang X, Kim SY, Kloepfer AM, Hinkle G, et al. A lentiviral RNAi library for human and mouse genes applied to an arrayed viral high-content screen. Cell 2006;124:1283–98.
27. Lerin C, Rodgers JT, Kalume DE, Kim SH, Pandey A, Puigserver P. GCN5 acetyltransferase complex controls glucose metabolism through transcriptional repression of PGC-1alpha. Cell Metab 2006;3:429–38.
28. Gerald D, Berra E, Frapart YM, Chan DA, Giaccia AJ, Mansuy D, et al. JunD reduces tumor angiogenesis by protecting cells from oxidative stress. Cell 2004;118:781–94.
29. Guzy RD, Hoyos B, Robin E, Chen H, Liu L, Mansfield KD, et al. Mitochondrial complex III is required for hypoxia-induced ROS production and cellular oxygen sensing. Cell Metab 2005;1:401–8.
30. Gao P, Zhang H, Dinavahi R, Li F, Xiang Y, Raman V, et al. HIF-dependent antitumorigenic effect of antioxidants *in vivo*. Cancer Cell 2007;12:230–8.
31. Lim JH, Lee YM, Chun YS, Chen J, Kim JE, Park JW. Sirtuin 1 modulates cellular responses to hypoxia by deacetylating hypoxia-inducible factor 1alpha. Mol Cell 2010;38:864–78.
32. Dominy JE, Gerhart-Hines Z, Puigserver P. Nutrient-dependent acetylation controls basic regulatory metabolic switches and cellular reprogramming. Cold Spring Harb Symp Quant Biol 2011;76:203–9.
33. Dang CV. Links between metabolism and cancer. Genes Dev 2012;26:877–90.
34. Kong X, Wang R, Xue Y, Liu X, Zhang H, Chen Y, et al. Sirtuin 3, a new target of PGC-1alpha, plays an important role in the suppression of ROS and mitochondrial biogenesis. PLoS ONE 2010;5:e11707.
35. Cash TP, Pan Y, Simon MC. Reactive oxygen species and cellular oxygen sensing. Free Radic Biol Med 2007;43:1219–25.
36. Hamanaka RB, Chandel NS. Mitochondrial reactive oxygen species regulate hypoxic signaling. Curr Opin Cell Biol 2009;21:894–9.
37. Metallo CM, Gameiro PA, Bell EL, Mattaini KR, Yang J, Hiller K, et al. Reductive glutamine metabolism by IDH1 mediates lipogenesis under hypoxia. Nature 2012;481:380–4.
38. Fendt SM, Bell EL, Keibler MA, Olenchock BA, Mayers JR, Wasylenko TM, et al. Reductive glutamine metabolism is a function of the alpha-ketoglutarate to citrate ratio in cells. Nat Commun 2013;4:2236.

Published OnlineFirst May 8, 2014; DOI: 10.1158/0008-5472.CAN-13-2893-T

Cancer Research
The Journal of Cancer Research (1916–1930) | The American Journal of Cancer (1931–1940)

AACR American Association for Cancer Research

Targeting Mitochondrial Oxidative Metabolism in Melanoma Causes Metabolic Compensation through Glucose and Glutamine Utilization

Ji-Hong Lim, Chi Luo, Francisca Vazquez, et al.

Cancer Res 2014;74:3535-3545. Published OnlineFirst May 8, 2014.